

## Limited variability in the phytoplankton *Emiliana huxleyi* since the pre-industrial era in the Subantarctic Southern Ocean

A.S. Rigual-Hernández<sup>a,\*</sup>, J.M. Sánchez-Santos<sup>b</sup>, R. Eriksen<sup>c,d</sup>, A.D. Moy<sup>e,f</sup>, F.J. Sierro<sup>a</sup>, J.A. Flores<sup>a</sup>, F. Abrantes<sup>g,h</sup>, H. Bostock<sup>i</sup>, S.D. Nodder<sup>j</sup>, A. González-Lanchas<sup>a</sup>, T.W. Trull<sup>c,d,e</sup>

<sup>a</sup>Área de Paleontología, Departamento de Geología, Universidad de Salamanca, 37008 Salamanca, Spain

<sup>b</sup>Departamento de Estadística, Universidad de Salamanca, 37008 Salamanca, Spain

<sup>c</sup>CSIRO Oceans and Atmosphere, Hobart, Tasmania 7001, Australia

<sup>d</sup>Institute for Marine and Antarctic Studies, University of Tasmania, Private Bag 129, Hobart, Tasmania 7001, Australia

<sup>e</sup>Antarctic Climate and Ecosystems Cooperative Research Centre and Australian Antarctic Program Partnership, University of Tasmania, Hobart, Tasmania 7001, Australia

<sup>f</sup>Australian Antarctic Division, Channel Highway, Kingston, Tasmania 7050, Australia

<sup>g</sup>Portuguese Institute for Sea and Atmosphere (IPMA), Divisão de Geologia Marinha (DivGM), Rua Alferedo Magalhães Ramalho 6, Lisboa, Portugal

<sup>h</sup>CCMAR, Centro de Ciências do Mar, Universidade do Algarve, Campus de Gambelas, 8005-139 Faro, Portugal

<sup>i</sup>School of Earth and Environmental Sciences, University of Queensland, Brisbane, Queensland 4072, Australia

<sup>j</sup>National Institute of Water and Atmospheric Research, Wellington 6021, New Zealand

### ARTICLE INFO

#### Article history:

Received 22 May 2020

Received in revised form 20 July 2020

Accepted 21 July 2020

Available online 24 July 2020

#### Keywords:

CO<sub>2</sub> emissions  
ocean acidification  
environmental change  
Southern Ocean  
coccolithophores  
*Emiliana huxleyi*

### ABSTRACT

The Southern Ocean is warming faster than the average global ocean and is particularly vulnerable to ocean acidification due to its low temperatures and moderate alkalinity. Coccolithophores are the most productive calcifying phytoplankton and an important component of Southern Ocean ecosystems. Laboratory observations on the most abundant coccolithophore, *Emiliana huxleyi*, suggest that this species is susceptible to variations in seawater carbonate chemistry, with consequent impacts in the carbon cycle. Whether anthropogenic environmental change during the industrial era has modified coccolithophore populations in the Southern Ocean, however, remains uncertain. This study analysed the coccolithophore assemblage composition and morphometric parameters of *E. huxleyi* coccoliths of a suite of Holocene-aged sediment samples from south of Tasmania. The analysis suggests that dissolution diminished the mass and length of *E. huxleyi* coccoliths in the sediments, but the thickness of the coccoliths was decoupled from dissolution allowing direct comparison of samples with different degree of preservation. The latitudinal distribution pattern of coccolith thickness mirrors the latitudinal environmental gradient in the surface layer, highlighting the importance of the geographic distribution of *E. huxleyi* morphotypes on the control of coccolith morphometrics. Additionally, comparison of the *E. huxleyi* coccolith assemblages in the sediments with those of annual subantarctic sediment trap records found that modern *E. huxleyi* coccoliths are ~2% thinner than those from the pre-industrial era. The subtle variation in coccolith thickness contrasts sharply with earlier work that documented a pronounced reduction in shell calcification and consequent shell-weight decrease of ~30–35% on the planktonic foraminifera *Globigerina bulloides* induced by ocean acidification. Results of this study underscore the varying sensitivity of different marine calcifying plankton groups to ongoing environmental change.

© 2020 The Authors. Published by Elsevier Ltd. This is an open access article under the CC BY-NC-ND license (<http://creativecommons.org/licenses/by-nc-nd/4.0/>).

### 1. Introduction

*Emiliana huxleyi* (Lohmann) Hay and Mohler is the most abundant and ubiquitous calcareous phytoplankton species and the only coccolithophore that regularly forms blooms in a wide range of environments, from polar to tropical systems and from

neritic to oceanic waters (Brown and Yoder, 1994; Tyrrell and Young, 2009). These blooms annually cover an areal extent of approximately  $1.0 \times 10^6$  km<sup>2</sup> equivalent to 0.28% of the global ocean (Brown and Yoder, 1994) and reach cell concentrations up to 10<sup>8</sup> cell per litre (Berge, 1962), thereby playing an important role in the marine carbon cycle (Westbroek et al., 1989). The underlying reason for the ecological success of *E. huxleyi* is due to its extensive genomic variability and consequent physiological adaptation repertoires (Read et al., 2013). Indeed, the high intraspecific

\* Corresponding author.

genetic divergence strongly suggests that *E. huxleyi* most likely represents a species complex, i.e. clades that are well separated according to most species definitions but are not always morphologically distinguishable (Read et al., 2013).

Carbon dioxide (CO<sub>2</sub>) emissions from anthropogenic sources have been altering the physical and chemical properties of the oceans beyond their natural state since the onset of the industrial era (Pachauri et al., 2014). In addition to increased warming, shallowing of mixed layers and changes in nutrient supply, enhanced oceanic uptake of anthropogenic CO<sub>2</sub> is lowering surface water pH and carbonate ion concentration, a process known as ocean acidification (Caldeira and Wickett, 2003). Ocean-carbon cycle models project that polar and subpolar ecosystems will be the first regions to become undersaturated with respect to calcium carbonate minerals in the coming decades (Orr et al., 2005; Feely et al., 2009). In particular, the mild alkalinity and low temperatures of the surface waters of the Southern Ocean, makes this region particularly vulnerable to ocean acidification (Cao and Caldeira, 2008; Fabry et al., 2009a; Shadwick et al., 2015).

Increased seawater acidification in laboratory experiments often results in reduced calcification rates in many calcified marine organisms, including planktonic foraminifera (Bijma et al., 2002), pteropods (Bednaršek et al., 2014; Manno et al., 2017), cold-water corals (Fabry et al., 2009b) and coccolithophorids (Meyer and Riebesell, 2015). Seawater carbonate chemistry manipulation experiments with *E. huxleyi* strains have come to different conclusions, with some studies pointing to enhanced calcification rates and net primary production at elevated partial pressure of CO<sub>2</sub> (pCO<sub>2</sub>) (e.g. Iglesias-Rodríguez et al., 2008), while others reported opposing effects (Riebesell et al., 2000). Reconciliation of these apparently conflicting findings is likely the result of the differing sensitivity to ocean acidification of the *E. huxleyi* strains employed in each study (Langer et al., 2009), including the possibility of contrasting positive responses to increased CO<sub>2</sub> availability versus negative responses to acidification (Bach et al., 2015). This notion is supported by Müller et al. (2015), who observed differing responses of three selected *E. huxleyi* strains isolated from the Southern Ocean to changing seawater carbonate chemistry. While laboratory experiments provide invaluable information of the physiological response of *E. huxleyi*, they also pose important limitations. The short duration of most laboratory manipulations preclude evolutionary adaptation to changing conditions (Langer et al., 2006; Schlüter et al., 2014), while the use of single isolated *E. huxleyi* strains eliminates the possibility of dominance shifts in the assemblage. These limitations introduce important uncertainties when extrapolating laboratory results to the natural field environment. It is, therefore, critical to perform field experiments (e.g. Triantaphyllou et al., 2018) to confirm or disprove the laboratory observations.

Comparison of sediment trap records with microplankton assemblages preserved in sea-floor sediments provides a valuable approach to assess the impact of climate change on plankton communities since the pre-industrial era (e.g. Jonkers et al., 2019). Moored time-series sediment traps are a reliable tool to reconstruct the seasonal cycles of specific plankton groups, including coccolithophores (e.g. Broerse et al., 2000b; Ziveri et al., 2000; Triantaphyllou et al., 2010, among others). Importantly, sediment trap records provide a resource to integrate annual coccolith fluxes and can be used to eliminate the effects of seasonality, therefore providing an important advantage versus plankton tows. These characteristics make annual sediment trap records a robust proxy for determining the state of modern coccolithophore communities. Similarly, coccolith assemblages from the uppermost layers of the sea-floor sediments represents an integrated assemblage of the past hundreds to thousands of years and therefore provides a baseline of the natural state of coccolithophore communities

before substantial human influences on the global environment. Together, the comparison of annual coccolith flux records with the assemblages preserved in the surface sediments provide a powerful means to assess changes in coccolithophore communities in response to ongoing environmental change.

The present study was partly prompted by earlier results from a field experiment comparing the weight of the planktonic foraminifera species *Globigerina bulloides* collected by sediment traps with those from the Holocene-aged sediments in the Australian sector of the Subantarctic Zone (Moy et al., 2009). Results from the latter study showed that modern *G. bulloides* populations are about 30–35% lighter than those in the Holocene sediments suggesting that ocean acidification could have caused a thinning of their shells. Following this approach, here we compare the annual coccolith assemblages of the key-stone species *E. huxleyi* collected by sediment traps deployed in the subantarctic surface waters south of Tasmania from an earlier study (Rigual-Hernández et al., 2020a) with a suite of Holocene-aged sediments samples retrieved in the same region. We characterized the coccolithophore assemblages in the sediment samples and determined the mass, length, and degree of calcification of *E. huxleyi* coccoliths, in order to answer the following research questions: (1) How do the seafloor sediments south of Tasmania preserve the record of the coccolith assemblages living during the pre-industrial era?; (2) Which and how natural and/or anthropogenic alterations to the marine environment, if any, have induced a change in the subantarctic *E. huxleyi* populations since the pre-industrial Holocene?; (3) How do any observed changes differ from those previously documented in planktonic foraminifera, the other major pelagic calcifiers in the Southern Ocean?

### 1.1. Oceanographic setting

The physical and chemical characteristics of the surface waters south of Tasmania exhibit pronounced latitudinal changes that occur as a series of steps or oceanographic fronts from north to south (Fig. 1). The Subtropical Front is characterized by a pronounced sea surface temperature gradient of approximately 4 °C that occurs in less than 0.5° of latitude (Rintoul et al., 1997) and represents the boundary between the subtropical gyres to the north and the Subantarctic Zone waters to the south. The Subantarctic Zone displays surface water pCO<sub>2</sub> well below atmospheric equilibrium, therefore acting as a large net sink for atmospheric CO<sub>2</sub> (~1 Gt C yr<sup>-1</sup>; Metzl et al., 1999; Lenton et al., 2013).

North of the Subtropical Front, the Zeehan current (an extension of the Leeuwin current) flows down the Tasmanian west coast (Ridgway, 2007). Along the east coast of Tasmania, an extension of the East Australian Current flows southward. Most of the East Australian Current extension that reaches south of Tasmania, is directed northwest as part of the Flinders Current, while the remaining flows poleward forming eddies (van Sebille et al., 2012; Pardo et al., 2019). South of the Subtropical Front, the general circulation is governed by the Antarctic Circumpolar Current that flows eastward connecting each of the major ocean basins (Rintoul et al., 2001). As a result of the different properties of the surface waters, the Subtropical and Subantarctic Zones exhibit different phytoplankton compositions (Odate and Fukuchi, 1995; Kopczynska et al., 2001; Eriksen et al., 2018).

The solubility of calcium carbonate minerals increases at lower seawater temperature and higher pressures, and thus their solubility increases with depth in the water column. Calcium carbonate preservation is largely controlled by changes in the carbonate ion concentration ([CO<sub>3</sub><sup>2-</sup>]) throughout the water column. The lysocline or saturation horizon is defined as the

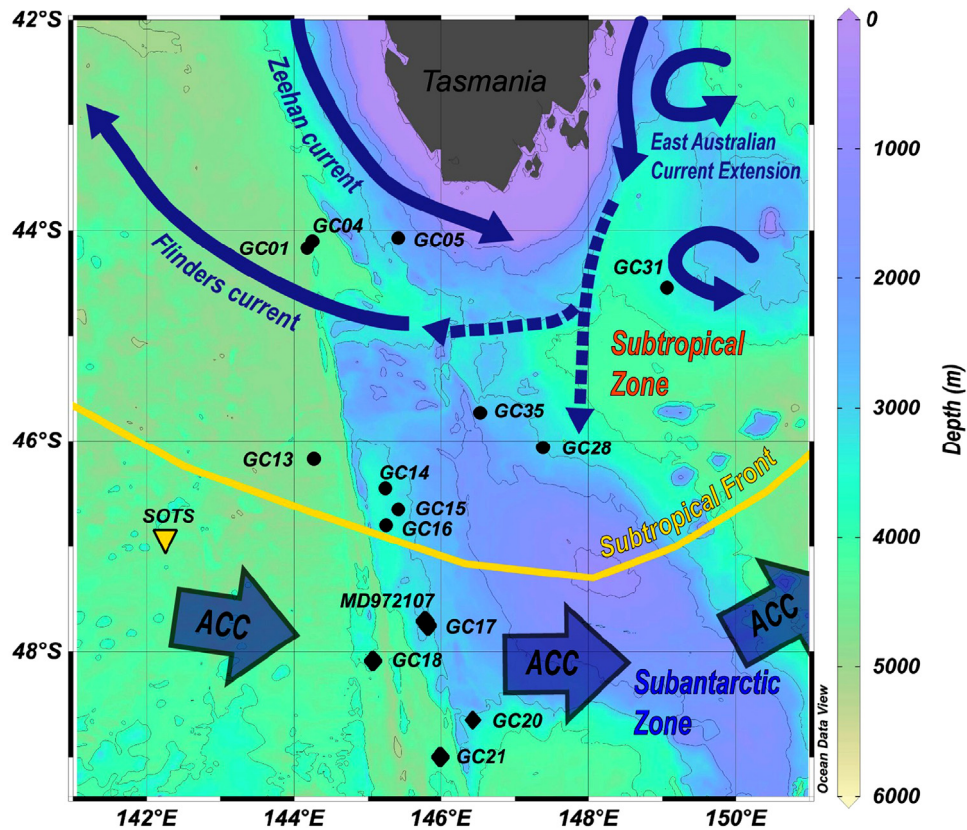


**Fig. 1.** Bathymetric map showing the location of Southern Ocean Time Series (SOTS) observatory sediment traps (yellow triangle) and Holocene core-top samples in the Subtropical Zone (black circles) and Subantarctic Zone (black diamonds) used in this study. Abbreviation: ACC – Antarctic Circumpolar Current. Oceanic fronts after Orsi et al. (1995). Ocean Data View software (Schlitzer, 2018) was used to generate this figure. Bathymetric data from General Bathymetric Chart of the Oceans (2020) (doi:10.5285/a29c5465-b138-234d-e053-6c86abc040b9).

depth in the water column where undersaturation ( $\Omega = 1$ ) with respect to a given  $\text{CaCO}_3$  phase (aragonite or calcite) occurs, therefore resulting in a pronounced increase in the rate of  $\text{CaCO}_3$  dissolution of that phase. In the subantarctic waters south of Tasmania, the calcite saturation horizon occurs at  $\sim 3400$  m (Moy et al., 2009; Bostock et al., 2011).

## 1.2. Distribution of *Emiliania huxleyi* morphotypes in the Southern Ocean

Based on the dimensions and fine structure of its coccoliths, *E. huxleyi* can be divided into different morphotypes. However, their precise delimitation can be difficult in some cases due to their overlapping features and size ranges (Young et al., 2003; Cook et al., 2011; Hagino et al., 2011). In the Southern Ocean, *E. huxleyi* largely dominates coccolithophore populations, displaying maximum abundances in the Subantarctic Zone and a general decline in its numbers moving poleward (Findlay and Giraudeau, 2000; Saavedra-Pellitero et al., 2014; Patil et al., 2017; Rigual Hernández et al., 2018). *E. huxleyi* populations in the waters south of Tasmania are primarily composed of three morphotypes: A overcalcified (A o/c), A and B/C (Cubillos et al., 2007; Cook et al., 2011; Cook et al., 2013), each of which is characterized by distinct coccolith structure and mass, photosynthetic pigment composition and differing responses to seawater carbonate chemistry variations (Cook et al., 2011; Cook et al., 2013; Krueger-Hadfield et al., 2014; Müller et al., 2015). These three morphotypes display important differences in their latitudinal distribution in the Australian sector of the Southern Ocean (Cubillos et al., 2007). The heavily-calcified type A o/c dominates *E. huxleyi* populations north of  $48^\circ\text{S}$  (i.e.

approximately the position of the Subantarctic Front), while the typical morphotype A extends roughly from the Subtropical Front to the Polar Front ( $\sim$ from  $44$  to  $55^\circ\text{S}$ ). Morphotype B/C displays the most southward distribution dominating from  $48$  to  $65^\circ\text{S}$  and becoming the only morphotype found in Antarctic Zone waters (Cubillos et al., 2007; Rigual Hernández et al., 2018). The light and delicate type B/C coccoliths are produced by the *E. huxleyi* var. *aurorae* ecotype, a Southern Ocean specialist with physiological adaptations that enable growth at cold temperatures ( $\sim 4^\circ\text{C}$ ) and low-light conditions (Cook et al., 2011).

## 2. Material and methods

### 2.1. The SOTS observatory

The Southern Ocean Time Series (SOTS) observatory is located at  $46^\circ 56' \text{S}$  and  $142^\circ 15' \text{E}$  (Fig. 1) and can be considered representative of a large swath of the Indian and Pacific sectors of the Subantarctic Zone ( $\sim 90$  to  $140^\circ\text{E}$ ; Trull et al., 2010). The SOTS facility consists of a set of three moorings platforms dedicated to measuring a range of physical, chemical, and biological processes, and the collection of ocean particles (Trull et al., 2010; Eriksen et al., 2018).

Rigual-Hernández et al. (2020a) analysed the seasonal variability of *E. huxleyi* coccolith assemblages collected by three vertically-moored sediment traps deployed from November 2009 to November 2010, to determine the seasonal variations of coccolith size and mass. Here, we take advantage of this study to obtain an approximation of the modern coccolithophore assemblages dwelling in the Subantarctic Zone. The potential source area (also

termed “statistical funnel”; Siegel et al., 1990; Siegel and Deuser, 1997) for the particles intercepted by a given sediment trap increases with depth. Therefore, to obtain the most robust representative of the modern conditions of Subantarctic Zone the three vertically-moored sediment trap records are represented as one composite sample (see section 2.6).

## 2.2. Holocene sediment samples

The sediment samples were retrieved from sediments underlying the subtropical and subantarctic waters south of Tasmania during the Australian Geological Survey Organisation Cruise 147 and IMAGES III cruise (Fig. 1 and Table 1). Most of the samples were collected from the South Tasman Rise, a large submarine plateau (approximately 500 km long) lying at depths ranging from 1000 to 4000 m. The majority of the samples were collected from locations above the top of the calcite saturation horizon and consequently expected to have good coccolith preservation. Based on the dated cores, sedimentation rates through the Holocene in the study area were low, with values ranging between 2–5 cm ky<sup>-1</sup>. The dated sediment samples suggest that the surface layer range between 3 to 7 kyrs BP (AMS <sup>14</sup>C dates for GC04 at a depth of 5–8 cm is 3160 yr BP, GC14 at 5–7 cm is 7373 yr BP (Connell and Sikes, 1997) and GC17 at 0–2 cm is 4440 yr BP (Moy et al., 2009)) therefore containing coccolithophore assemblages sedimented during the pre-industrial Holocene era.

## 2.3. Sample processing for calcareous nannoplankton analysis

Samples for calcareous nannoplankton analysis were prepared following a method adapted from Flores and Sierro (1997). Approximately 50 mg of dry sediment were suspended in a solution of sodium carbonate and sodium hydrogen carbonate (pH 8) with ammonia (2%). The samples were subject to gentle mechanical disaggregation on a rotating carousel for 24 hours (Stoll and Ziveri, 2002). Between 0.2 and 2 ml of sample were extracted with a micropipette and dropped onto a petri dish filled with buffered water and with a cover slip in its bottom. After settling 12 hours, the excess of water was removed using filter-paper strips. Then the cover slip was left to dry and mounted on a glass slide with Canada balsam. Coccoliths were identified to species level using a Nikon Eclipse 80i polarised light microscope at 1000x magnification. A minimum of 300 coccoliths were identified to the lowest taxonomic level possible. Only in GC18 sample, that contained extremely low coccolith abundance this target was not met, with only 45 coccoliths identified. Then, coccolith relative and absolute abundances were estimated.

A Carl Zeiss EVO HD25 Scanning Electron Microscope (SEM) was used to identify and classify about 100 *E. huxleyi* coccoliths per sample into morphotypes. Round glass cover slips were prepared following Flores and Sierro (1997), mounted on aluminium stubs and coated with gold. *E. huxleyi* morphotypes were identified following the same criteria as Rigual-Hernández et al. (2020a) which in turn is based on Young et al. (2003) and Hagino et al. (2005) with slight modifications adapted for Southern Ocean populations. Coccolithophore assemblage composition of most of the sediment samples analysed here had been previously characterized by Findlay and Giraudeau (2002). However, in order to be consistent and make the results comparable with the sediment trap results all the samples were recounted.

## 2.4. The *Calcidiscus leptoporus* – *Emiliania huxleyi* Dissolution Index (CEX)

Modern coccolith sinking assemblages in the subantarctic waters south of Tasmania are dominated by *E. huxleyi* (> 80% of the annual sinking assemblage) followed by *Calcidiscus leptoporus* (~10%) (Rigual-Hernández et al., 2020b). Although the coccoliths of these two species are placoliths, i.e. they are composed of a proximal and distal shield connected by a central column, they represent the two ends of the coccolith dissolution spectrum. While *E. huxleyi* produces fragile coccoliths with delicate T-shaped elements that make them particularly vulnerable to dissolution, and *C. leptoporus* producing heavily calcified shields highly resistant to dissolution. Since *E. huxleyi* and *C. leptoporus* have relatively similar ecological affinities, changes in this ratio could be potentially used as indicator of the intensity of dissolution in the sediments (e.g. Dittert et al., 1999; Boeckel and Baumann, 2004). If it is assumed that the proportion of these two species has remained similar through the Holocene until present, the *C. leptoporus* – *E. huxleyi* Dissolution Index (CEX) (Dittert et al., 1999) could be used to assess dissolution in the sediments. Previously, a ratio of 0.6 has been proposed as the critical boundary below which substantial carbonate dissolution occurs (Dittert et al., 1999; Boeckel and Baumann, 2004). The CEX index is calculated as follows:

$$CEX = \%E. huxleyi / (\%E. huxleyi + \%C. leptoporus)$$

## 2.5. Coccolith mass and size measurements

A minimum of 100 *Emiliania huxleyi* coccoliths were analysed in all samples with exception of GC16 and GC18 where 90 and 65 coccoliths were measured, respectively. A total of 1128 fields of view (FOV) were photographed using a Nikon Eclipse LV100 POL

**Table 1**  
Summary of zonal system, latitude, longitude and water column depth of the sediment samples. STZ – Subtropical Zone, SAZ – Subantarctic Zone.

Core ID	Zonal system	Longitude (°E)	Latitude (°S)	Water column depth (m)
GC01	STZ	144.18	44.17	4262
GC04	STZ	144.25	44.10	2980
GC05	STZ	145.42	44.07	2334
GC13	STZ	144.27	46.17	4452
GC14	STZ	145.24	46.45	3360
GC15	STZ	145.42	46.65	3260
GC16	STZ	145.25	46.80	3523
GC17	SAZ	145.82	47.75	3001
GC18	SAZ	145.07	48.09	4368
GC20	SAZ	146.43	48.65	3300
GC21	SAZ	145.99	49.00	4132
GC28	STZ	147.38	46.06	3065
GC31	STZ	149.06	44.55	3402
GC35	STZ	146.53	45.73	2720
MD972107	SAZ	145.78	47.71	2950

microscope equipped with circular polarisation and a Nikon DS-Fi1 8-bit colour digital camera. C-Calcita software (Fuertes et al., 2014) extracted images of all particles between 1 and 8  $\mu\text{m}$  from each FOV photograph. Then, the output files of single *E. huxleyi* coccoliths were visually selected. *E. huxleyi* coccoliths were differentiated from *Gephyrocapsa* species – the other members of Noëlaerhabdaceae family present in the Subantarctic Zone with relatively similar coccolith dimensions– on the basis of the presence or absence of a conjunct bridge. Even when this bridge is missing, *Gephyrocapsa* coccoliths often display two conspicuous highly calcified thickenings that correspond with the base of the bridge allowing identification of members of this genus. Coccolith mass and length measurements on the output images of *E. huxleyi* coccoliths were performed automatically by C-Calcita software. Further details of the calibration and image analysis protocol can be found in Rigual-Hernández et al. (2020a).

The proportions between different morphometric parameters of a coccolith of a given species typically vary with size (i.e. allometric growth; Young and Ziveri, 2000). In particular, coccolith thickness has been documented to increase in proportion to its size (O’Dea et al., 2014). Therefore, in order to compare coccolith thickness across datasets beyond this relationship we calculated the size-normalized coccolith thickness, hereinafter SN thickness after O’Dea et al. (2014) and Bolton et al. (2016) using the following formula:

$$\text{SN thickness} = \text{CT} + [(\text{ML} - \text{DSL}) \times \text{S}]$$

where the first term, CT, is the coccolith thickness of coccolith A in sample X and the correction for size is given by the second term, in which ML is the mean coccolith length of all the samples analysed together (i.e. sediment trap plus sediment samples), DSL (distal shield length) is the length of *E. huxleyi* coccolith A in sample X, and S is the slope of the regression line between coccolith length (x axis) and thickness (y axis) in sample X.

## 2.6. Statistical Analyses

As the variables coccolith mass, DSL and SN thickness have a weighted composition, the weighted Kolmogorov-Smirnov test (Monahan, 2011) was performed instead of the classical test (Darling, 1957) to assess the difference in *E. huxleyi* coccolith mass, DSL and SN thickness between modern (Sediment trap) and pre-industrial (Holocene sediments) datasets. Since the sediment traps were deployed in the Subantarctic Zone, we also performed a second comparison with Subantarctic Zone seabed samples only – i.e. excluding all the sediment samples retrieved from the Subtropical Zone. The Kolmogorov-Smirnov comparison consists of a two-sample distribution-free test designed to identify possible deviations from the initial hypothesis that the distributions of the two compared populations are identical. If the p value is small, i.e. 0.05 or less, it can be concluded that the distributions of the two populations compared are significantly different.

The modern subantarctic assemblage, termed “sediment trap composite sample” was derived by integrating the coccolith flux time series collected during a year (from August 2011 until July 2012) from three vertically moored sediment traps placed at 1000, 2000 and 3800 m at the SOTS site from a previous study (Rigual-Hernández et al., 2020a). Since the relative abundance of *E. huxleyi* morphotypes display substantial latitudinal variations across the subtropical and subantarctic waters south of Tasmania (Findlay and Giraudeau, 2000; Cubillos et al., 2007) and each of these morphotypes are characterized by coccoliths with different degree of calcification and size ranges, we ran two different comparisons between the “sediment trap composite sample” and sediments: one with the whole sediment sample dataset – hereinafter termed

“sea-bed sediment group” – dataset and one with the subantarctic sediment samples only, hereinafter termed “subantarctic sediment group”.

Additionally, the Pearson’s correlation (Pearson, 1907) used to assess the degree of association between *E. huxleyi* morphometric parameters, CEX, latitude and water column depth of the seafloor samples.

## 3. Results

### 3.1. Coccolith assemblage composition and CEX index

With the exception of GC13, GC14, GC16 and GC18, the calcareous nannofossil assemblages were largely dominated by *E. huxleyi* that accounted for between 60 and 84% of the assemblage, followed by *C. leptoporus* (1–23%) and *Gephyrocapsa* group (including *G. muelleriae*, *G. oceanica*, *Gephyrocapsa* spp. < 3  $\mu\text{m}$  and *Gephyrocapsa* spp. > 3  $\mu\text{m}$ ; 4–28%) (Supplementary Table 1). GC13, GC14, GC16 and GC18 are among the samples retrieved from deepest locations and exhibit more pronounced signs of dissolution. These samples were dominated or co-dominated by the heavily calcified *C. leptoporus* (7–42%) and *Coccolithus pelagicus* (8–42%).

CEX values in most sediment samples were above 0.6 (Dittert et al., 1999; see also section 2.6), suggesting that post-depositional dissolution processes had not altered the composition of the coccolith assemblages. Only in samples GC13, GC16 and GC18 CEX was equal or below the 0.6 threshold, indicating that carbonate dissolution could have compromised the imprint of some taxa. CEX exhibited a significant correlation with water column depth ( $r = -0.66$ ,  $p < 0.01$ ,  $n = 15$ ) (Fig. 2) highlighting the intimate relationship between depth and calcite dissolution (Milliman, 1975). Note that the slightly different r coefficients between CEX and depth shown in Figs. 2 and 5 are due to the different number of samples used in each correlation.

### 3.2. Morphotype composition of *E. huxleyi* assemblages

Overall, SEM analyses on the Holocene sediment samples revealed that most of the *E. huxleyi* coccoliths were affected by dissolution. The total or partial loss of their T-elements and central area elements (e.g. Fig. 3a) precluded the identification to morphotype level of about 85% (average value) of the *E. huxleyi* coccoliths found in the sediment samples (Fig. 4 and Supplementary Table 2). GC05 and GC04 exhibited the best preservation with 49 and 37 % of the *E. huxleyi* coccoliths identifiable to morphotype

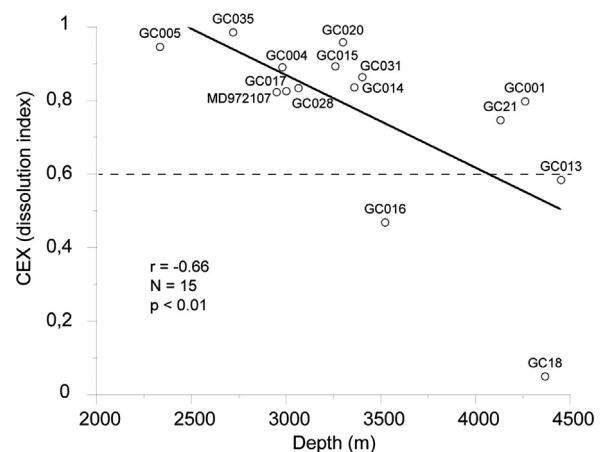
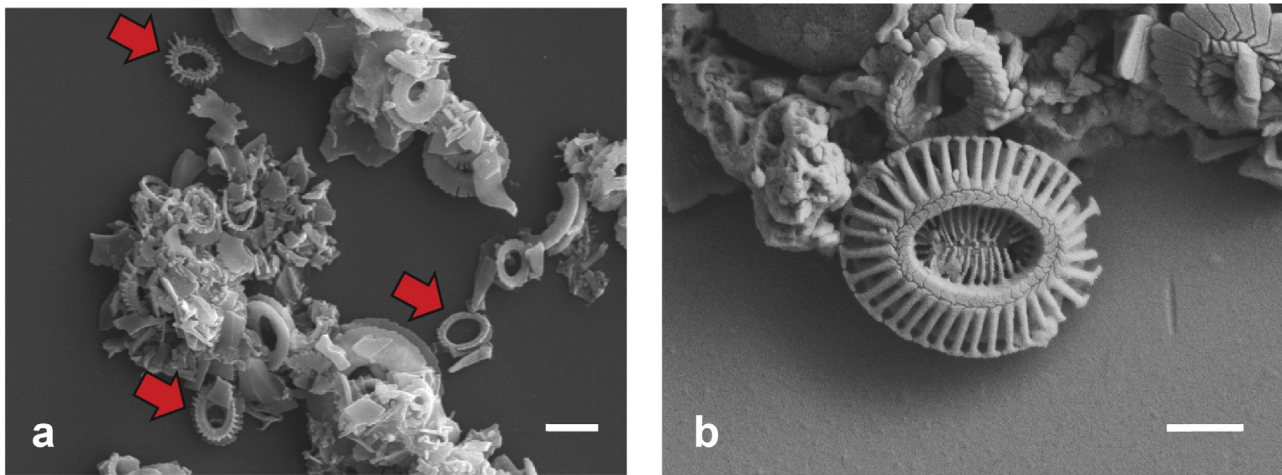
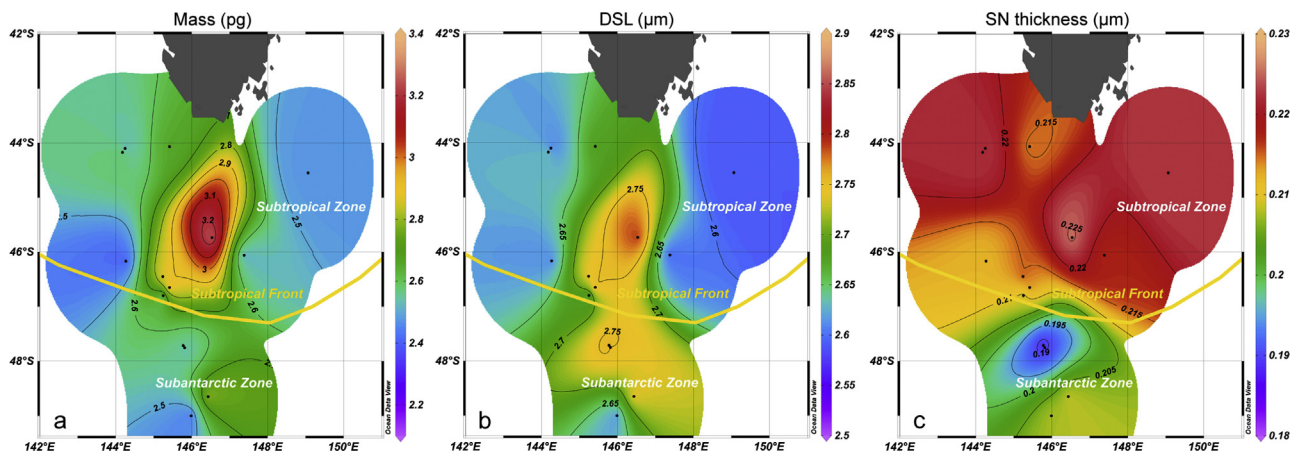


Fig. 2. Regression plot between the CEX index (*Calcidiscus leptoporus* – *Emiliania huxleyi* Dissolution Index) and water column depth of the sediment samples.



**Fig. 3.** Scanning Electron Microscope photographs showcasing the two ends of the preservation spectrum of *E. huxleyi* coccoliths in the sediments south of Tasmania: highly dissolved coccoliths (red arrows) (a) and well-preserved coccolith (type A) (b). Scale bars: a = 2  $\mu\text{m}$ ; b = 1  $\mu\text{m}$ .



**Fig. 4.** Relative abundance of *E. huxleyi* morphotype in (a) the Holocene sediments south of Tasmania in latitudinal order from north (left) to right (south) and (b) in the subantarctic SOTS sediment traps (composite sample grouping the three sediment traps). B/C and C morphotypes grouped together under B/C.

level. These two samples correspond to the northernmost locations of data set and displayed the highest concentrations of type A (29 and 22% for GC05 and GC04, respectively) and among the highest for type A o/c (13 and 15%) of the total coccoliths counted, in all samples (Fig. 4). In contrast the poorest preservation was observed in the subantarctic – and second deepest sample (depth 4368 m) – GC18, that was almost barren for *E. huxleyi* coccoliths. Very poor coccolith preservation was also documented in the samples located in GC13, GC14, GC15 and GC16 located in the western flank of the South Tasman Rise where > 98% of the *E. huxleyi* coccoliths were unidentifiable (Fig. 4). The poor preservation of the *E. huxleyi* coccoliths in the sediments contrasts with their good conservation in the SOTS sediment trap samples, where all coccoliths found in distal shield view were identifiable (Rigual-Hernández et al., 2020a).

### 3.3. Coccolith mass, length, and thickness distributions in the sediments south of Tasmania

A total of 1794 *E. huxleyi* coccoliths from the Holocene sediments south of Tasmania were visually identified and analysed for morphometric parameters. An average of 128 coccoliths per sample were analysed, ranging from 65 in sample GC20 to 189 in GC04. Average coccolith mass in the sediments is  $2.65 \pm 1.20$  pg

(average  $\pm$  standard deviation). Peak values are observed in the subtropical samples GC35 and GC15 ( $3.34 \pm 1.50$  and  $3.29 \pm 1.49$  pg) collected from the northern flank of the South Tasman Rise and minima in the nearby, but deeper (3523 m), GC16 site ( $2.16 \pm 1.23$  pg) depth) and in GC21 ( $2.35 \pm 0.95$  pg), located the southern flank of the South Tasman Rise. The spatial distribution of coccolith mass in the sediments south of Tasmania was similar to that of DSL (Fig. 6 a and b), exhibiting a strong and significant correlation between both parameters ( $r = 0.86$ ; Fig. 5). Unlike coccolith mass and DSL, SN thickness exhibits a clear latitudinal gradient with maximum values observed in the subtropical samples GC31, GC01 and GC35 and minima in the subantarctic samples GC17 and MD972107 (Fig. 6c). SN thickness was not correlated with either coccolith mass or DSL ( $r = 0.36$  and  $-0.13$ , respectively), but was significantly negatively correlated with latitude ( $^{\circ}\text{S}$ ) ( $r = -0.61$ ; Fig. 5).

### 3.4. Coccolith morphometrics: sediment trap versus Holocene sediment *E. huxleyi* assemblages

Annual flux-weighted coccolith mass, DSL and SN coccolith thickness for the sediment trap composite sample are 2.76 pg, 2.82  $\mu\text{m}$  and 0.192  $\mu\text{m}$ , respectively. Comparison of the coccolith mass distributions between datasets initially suggests that modern

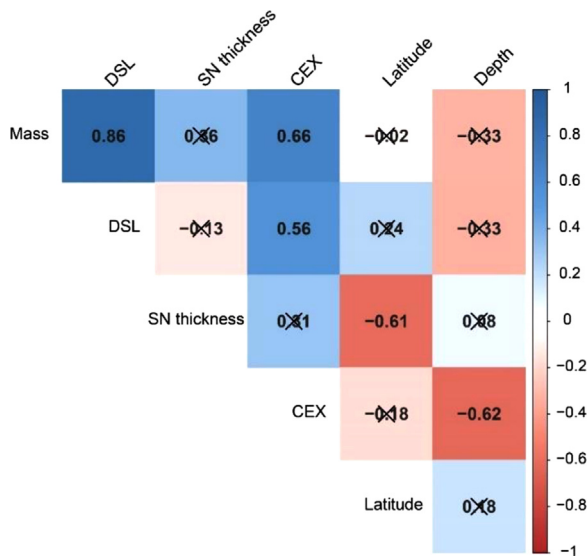


**Fig. 5.** Pearson correlation matrix for mean morphometric parameters of *E. huxleyi* coccoliths (mass, DSL and SN thickness), the dissolution index CEX, water column depth and latitude of the Holocene-aged sediment samples south of Tasmania. Non-significant correlations ( $p$  values  $> 0.05$ ) are crossed out.  $N = 14$  samples (no coccolith morphometric data for GC18).

*E. huxleyi* coccolith assemblages (i.e. those from the composite sediment trap sample) display a higher calcite content than their counterparts retrieved from the seafloor, both when all sediment samples are considered together, and when only subantarctic sediment samples are compared (Fig. 7a and b). For DSL distributions, the results of the Kolmogorov-Smirnov test yielded similar results to those for coccolith mass, with DSL of the sediment trap assemblages being greater than that of all the seafloor sediment samples (i.e. the sea-bed sediment group) and the subantarctic samples (Fig. 7c and d). Interestingly, the SN coccolith thickness comparison indicates that Holocene *E. huxleyi* populations were more calcified than modern ones (Fig. 7e). This statement holds true when we narrow the comparison to the subantarctic sediment group (Fig. 7f).

## 4. Discussion

### 4.1. Factors influencing the preservation and composition of coccolith sinking assemblages

The complex interaction of several physical, chemical and biological processes can alter the original coccolithophore assemblage since its initial production in the surface ocean until its eventual preservation in the sediments. Grazing by zooplankton is the first factor influencing the original coccolithophore assemblage produced in the surface layer and can have opposing effects on coccolith preservation. On the one hand, mechanical breakage of coccospheres and/or the effect of acidic food vacuoles (3–5 pH) of some zooplankton species may result in fragmentation of coccoliths and/or rapid calcite dissolution (e.g. Broerse et al., 2000a; Mayers et al., 2019). On the other hand, formation of faecal and algal aggregates can reduce the contact of the coccoliths with the environment and effectively increase their sinking rates, thereby facilitating their rapid transit through the water column and deposition on the seafloor (Ziveri et al., 2007). In the study area, Pearce et al. (2011) estimated that microzooplankton exerts a strong top-down control by removing about 80% of primary production during the austral summer, while Ebersbach et al. (2011) documented that the bulk of the particles sinking out of the mixed layer during summer occurs in the form of faecal aggregates. SEM observations indicate that the preservation of *E. huxleyi* coccoliths collected by the traps is excellent indicating that negligible dissolution occurs in the transit of the coccolithophores throughout the water column (Rigual-Hernández et al., 2020a). Taken together, all the above-mentioned studies suggest that grazing pressure in the subantarctic waters facilitates the rapid transit of coccoliths from the surface to the sea floor thereby optimizing their preservation. The good preservation of the coccoliths in the traps is consistent with Moy et al. (2009) who reported minimal dissolution of planktonic foraminifera *Globigerina bulloides* tests captured by sediment traps in the study region.

Once at the seabed, the accumulated coccoliths are exposed to several processes that can alter the preservation and composition of the original assemblage. Firstly, bioturbation can result in the mixing of sediment layers introducing a blurring effect on the information preserved in the sediment record (Boudreau, 1998). The AMS  $^{14}\text{C}$  dates (section 2.2) confirm that all the samples analysed here are Holocene (Connell and Sikes, 1997; Findlay and

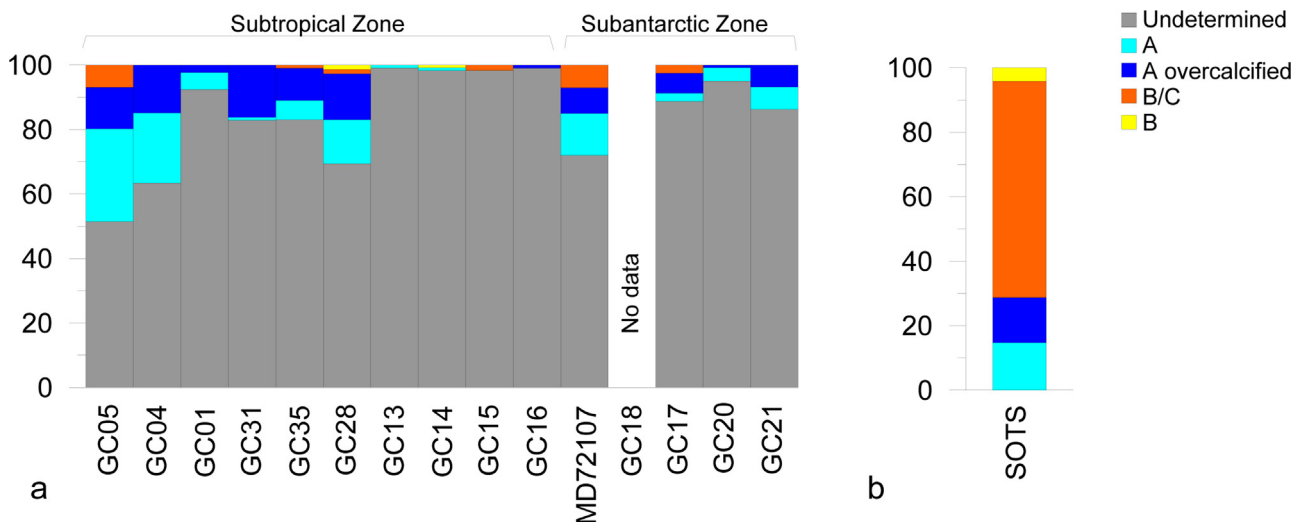


**Fig. 6.** Distribution of *E. huxleyi* coccolith mass (a), DSL (Distal Shield Length) (b) and SN thickness (c) in the seafloor Holocene sediments south of Tasmania. Black points identify location of sampling points. Ocean Data View software (Schlitzer, 2018) was used to generate this figure.

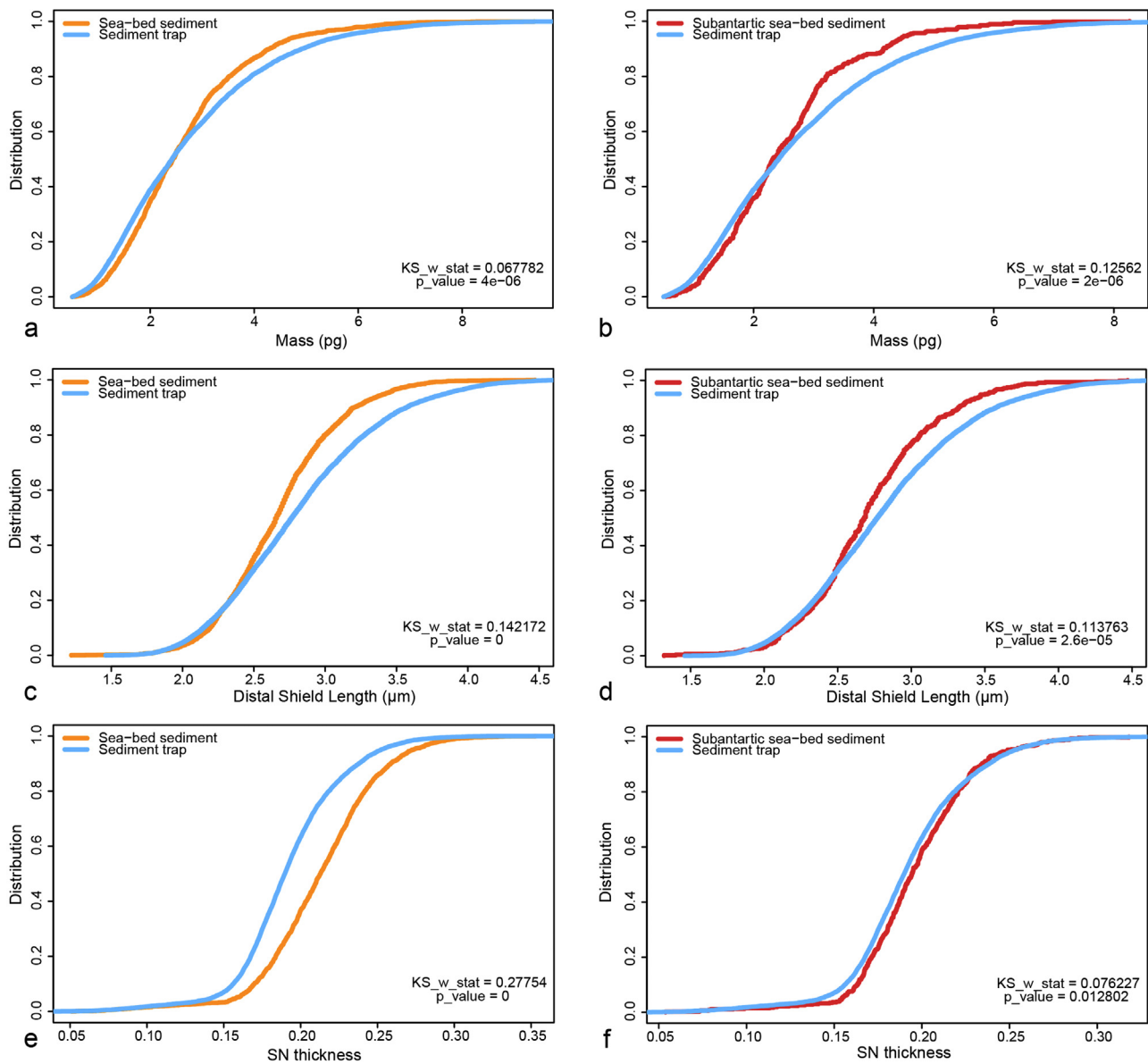


**Fig. 7.** Weighted Kolmogorov-Smirnov comparison of the distribution of *Emiliana huxleyi* coccolith mass, DSL and Size-Normalized (SN) coccolith thickness between: (i) sediment trap composite sample versus all sediment samples grouped together (a, c and e); (ii) and sediment trap composite sample versus subantarctic sediment samples grouped together (b, d and f).

Giraudeau, 2002; Moy et al., 2009). Secondly, carbonate dissolution is generally considered the most important factor altering the original coccolith assemblage. SEM observations indicate that most of the *E. huxleyi* coccoliths in all the sediment samples analysed have experienced a variable degree of dissolution and fragmentation of their elements and shields that precluded the identification to morphotype-level of a substantial number of coccoliths (Figs. 3 and 4). It is likely that supralysocline dissolution processes (Milliman et al. (1999) related to the guts and faeces of epipelagic grazers, and microbial oxidation of organic matter facilitated post depositional dissolution of the sea-floor samples.

#### 4.2. Biogeographical distribution patterns of *Emiliana huxleyi* coccoliths

The modern Subtropical and Subantarctic Zone waters host different proportions of *E. huxleyi* morphotypes, with type A and A o/c occurring more frequently in the Subtropical Zone, while the

subantarctic waters are dominated by morphotype B/C, endemic to the Southern Ocean (Cubillos et al., 2007). Notably, these morphotypes display important differences in their degree of calcification, with morphotype A and A o/c exhibiting substantially more calcified coccoliths than the weakly calcified type as reflected in their different coccolith shape factors ( $k_s = 0.04, 0.02$  and  $0.015$  for type A o/c, A and B/C, respectively; Young and Ziveri, 2000; Poulton et al., 2011). Therefore, we initially expected the *E. huxleyi* coccolith mass distributions in the sea floor to mirror the latitudinal gradient in the surface layer, displaying maximum coccolith mass in the northern stations and minima south of the Subtropical Front. The lack of a clear decreasing north-south gradient in both mass and length (Fig. 6a and b) is interpreted as resulting from substantial post depositional dissolution processes on the seafloor. This idea is supported by the significant correlations of coccolith mass and DSL with CEX (Fig. 5) suggesting that dissolution most likely altered these two parameters. In contrast, the SN thickness displays a clear latitudinal pattern



consistent with the distribution of morphotypes in the surface layer (Fig. 6) and is not correlated with the dissolution index CEX (Fig. 5). These observations suggest that the SN thickness is decoupled from coccolith preservation (O'Dea et al., 2014). Comparison of SN thickness distributions indicates that subtropical *E. huxleyi* coccoliths are 10% thicker than those preserved in the subantarctic sediments. We speculate that the variations in coccolith thickness along the latitudinal environmental gradient are intimately related to changes in the proportions of *E. huxleyi* morphotypes. Indeed, if we focus on the subtropical sample with the best preservation, i.e. sample GC05, the contribution of type A and type A o/c together accounts for ~40% of the assemblage (Fig. 4). And it is important to note that this value should be viewed as an underestimation because about half of the *E. huxleyi* coccoliths in sample GC05 were unidentifiable to morphotype level. Indeed, the contribution of type A and type A o/c together would increase up to 85% if the unidentified *E. huxleyi* coccoliths are not considered. Although the poor preservation of the *E. huxleyi* coccoliths in the subantarctic samples precludes estimation of morphotype proportions, previous research in the nearby New Zealand Subantarctic Zone indicates that type B/C is, by far the dominant morphotype in the surface sediments (Saavedra-Pellitero and Baumann, 2015). Taken together, all the above observations support the notion that changes in coccolith thickness along the north-to-south environmental gradient south of Tasmania are controlled by the morphotype composition of *E. huxleyi* populations.

#### 4.3. Comparison of modern and pre-industrial Holocene *Emilia* huxleyi assemblages

Given the substantial variability in morphotype composition of *E. huxleyi* assemblages between the subtropical and subantarctic waters south of Tasmania (Findlay and Giraudeau, 2000; Cubillos et al., 2007; Rigual-Hernández et al., 2020a), we focus on the comparison of the SOTS sediment traps with the subantarctic sediment samples (Fig. 7b, d and f) to assess the changes of *E. huxleyi* populations in the subantarctic region since the pre-industrial era.

Since the coccolithophore populations captured by the SOTS sediment traps and those from the subantarctic Holocene-aged sediment samples display CEX values above 0.7, it can be inferred that a negligible to low number of *E. huxleyi* coccoliths had been completely removed from these samples. In other words, the results suggest that the bulk of *E. huxleyi* coccoliths that reached the seafloor in the Subantarctic Zone are still present in the sediments, thereby discarding the possibility that differential dissolution removed the most weakly calcified *E. huxleyi* coccoliths from the seafloor. However, this does not imply that *E. huxleyi* coccoliths were unaltered by dissolution. In fact, the SEM observations clearly indicate that most of the *E. huxleyi* coccoliths in the sediments experienced a variable degree of CaCO<sub>3</sub> loss that resulted in a reduction of both coccolith mass and DSL. In contrast, the results of this study (see section 4.2), along with previous research (O'Dea et al., 2014), indicate that SN thickness is unaffected by dissolution, this parameter can be used to compare to sediment trap and seafloor coccolith assemblages on an equal footing.

Comparison of the distributions of SN thickness indicates that modern *E. huxleyi* coccoliths are less calcified than Holocene ones from the subantarctic sediments (Fig. 7f). It is important to note that although this difference is significant (at p-value < 0.05), it is small with modern *E. huxleyi* coccoliths being 2% thinner than pre-industrial Holocene ones. Next, we examine the most probable environmental factors that could have driven this change between the Holocene and present.

Several lines of evidence strongly suggest that temperature is a critical factor controlling the biogeographical distribution of *E. huxleyi* morphotypes in the Southern Ocean (Cubillos et al., 2007; Charalampopoulou et al., 2016; Rigual Hernández et al., 2018; Saavedra-Pellitero et al., 2019). In particular, unpublished results from Hallegraeff et al. (see Rigual-Hernández et al., 2020a for more information) have showed that Southern Ocean B/C strains are able to grow at 4, 10 and 17 °C, while types A and A o/c do not survive at 4 °C. Since the weakly calcified type B/C dominates the coccolithophore populations in the Subantarctic Zone, any substantial variation in water temperatures could potentially induce a change in the proportions of morphotypes, thereby driving a change in the average size and weight of the *E. huxleyi* populations (Bach et al., 2012). Sea surface temperature reconstructions based on alkenones of core GC17 (Fig. 1), indicate that surface temperatures in the Subantarctic Zone has decreased approximately 2.5 °C since the early Holocene (Sikes et al., 2009). Therefore, it is plausible that the warmer conditions during the early to mid Holocene (Sikes et al., 2009) favoured the development of *E. huxleyi* strains with affinity for higher SSTs, such as type A and A o/c (Cubillos et al., 2007; Cook et al., 2011), thereby explaining the thicker coccoliths recorded in the Holocene sediments. Moreover, seawater carbonate chemistry manipulation experiments with Southern Ocean *E. huxleyi* strains (corresponding to morphotypes B/C, A and A o/c) showed differing physiological responses to projected pCO<sub>2</sub> levels (Müller et al., 2015). In particular, type B/C was shown to be the most sensitive of the three morphotypes to high pCO<sub>2</sub>, almost ceasing calcification at pCO<sub>2</sub> levels above 1000 µatm. However, it is important to note that response of type B/C to increased pCO<sub>2</sub> was not linear, as it displayed an increase of up ~20% on its growth rates from pre-industrial pCO<sub>2</sub> concentrations (~250 µatm) to present industrial levels (~400 µatm) before reducing its growth rates at further higher pCO<sub>2</sub> concentrations. In turn, growth rates of type A strains remained constant between Holocene and industrial pCO<sub>2</sub> levels. Thus, it is possible that seawater carbonate chemistry changes in subantarctic waters induced by enhanced pCO<sub>2</sub> levels during the industrial era would have favoured the growth of B/C populations, thereby resulting in an overall ecologically-driven decrease in the calcification of subantarctic populations, as suggested by the results.

## 5. Conclusions

Comparison of the morphotype composition and morphometric parameters of *E. huxleyi* coccolith preserved in the Holocene-aged sediments south of Tasmania with assemblages from annual sediment-trap time series records permit answers to the research questions posed in this paper:

1- Results indicate that, whereas post depositional processes diminished the mass and distal shield length of *E. huxleyi* coccoliths preserved in the Holocene-aged sediments, the size normalized coccolith thickness is retained allowing comparison of modern and pre-industrial *E. huxleyi* assemblages using this variable.

2- Modern *E. huxleyi* populations in the Subantarctic Zone produce coccoliths about 2% thinner than those from the pre-industrial Holocene. This result suggests that ongoing anthropogenic-driven environmental change in the Subantarctic Zone has induced only minor changes in the composition or physiological response of *E. huxleyi* populations. The production of subtly thicker coccoliths during the pre-industrial Holocene attributable to the warmer conditions and/or lower pCO<sub>2</sub> levels could have possibly favoured the growth of *E. huxleyi* morphotypes other than the currently dominant, and weakly calcified, type B/C.

3- The limited variation in coccolith calcification of *E. huxleyi* since the pre-industrial era contrasts sharply with the 30–35% reduction in shell weight of the dominant class of calcifying zooplankton, foraminifera, as observed for the species *Globigerina bulloides* (Moy et al., 2009). Ocean acidification has been documented to have an overall negative effect on the calcification of both species (Meyer and Riebesell, 2015; Davis et al., 2017). However, the results of this study suggest that there are important differences in the sensitivity of both groups to the  $p\text{CO}_2$  increase since the onset of the industrial revolution (i.e. from  $\sim 250$  to  $\sim 400$   $\mu\text{atm}$ ) with *E. huxleyi* subantarctic strains being more resilient than *G. bulloides*.

Understanding the response of coccolithophores to environmental change is important to enable robust predictions of the impacts on higher trophic levels, and to carbon cycling on regional and global scales. While the results presented here indicate that critical ocean acidification thresholds for *E. huxleyi* calcification have not been reached, it is expected that they will be crossed in the coming decades (Müller et al., 2015). Moreover, recent research has provided evidence that less abundant but larger subantarctic coccolithophore species (such as *Calcidiscus leptoporus*) account for a greater fraction of  $\text{CaCO}_3$  export to the deep sea than *E. huxleyi* (Rigual-Hernández et al., 2020b). Therefore, it is of critical importance to maintain continuous sampling programs in key Southern Ocean locations and extend the monitoring to other ecologically important species to better evaluate the response of marine ecosystems to predicted environmental change.

#### Declaration of Competing Interest

The authors declare that they have no known competing financial interests or personal relationships that could have appeared to influence the work reported in this paper.

#### Acknowledgments

This project has received funding from the European Union's Horizon 2020 research and innovation programme under the Marie Skłodowska-Curie grant agreement number 748690 – SONAR-CO2 (ARH, JAF and FA). FA acknowledges FCT funding support through project UIDB/04326/2020. SN and HB were funded via the New Zealand Strategic Science Investment Fund to the 'Marine Geological Processes' programme in NIWA. The authors acknowledge the assistance of Vito Clericò and Enrique Diez (USAL-NANOLAB) in SEM analyses. Authors wish to thank José Ignacio Martín and Miguel Ángel Fuertes for their assistance in nannoplankton sample preparation and calibration of C-Calcita software, respectively. Authors would like to express our sincere thanks to two anonymous reviewers and editor Anne Chin for valuable comments that helped to improve the paper.

#### Appendix A. Supplementary data

Supplementary material related to this article can be found, in the online version, at doi:<https://doi.org/10.1016/j.ancene.2020.100254>.

#### References

- Bach, L.T., Bauke, C., Meier, K., Riebesell, U., Schulz, K.G., 2012. Influence of changing carbonate chemistry on morphology and weight of coccoliths formed by *Emiliania huxleyi*. *Biogeosciences* 9, 3449–3463.
- Bach, L.T., Riebesell, U., Gutowska, M.A., Federwisch, L., Schulz, K.G., 2015. A unifying concept of coccolithophore sensitivity to changing carbonate chemistry embedded in an ecological framework. *Progress in Oceanography* 135, 125–138.
- Bednaršek, N., Tarling, G.A., Bakker, D.C., Fielding, S., Feely, R.A., 2014. Dissolution dominating calcification process in polar pteropods close to the point of aragonite undersaturation. *PLoS one* 9, e109183.
- Berge, G., 1962. Discoloration of the sea due to *Coccolithus huxleyi* "bloom". *Sarsia* 6, 27–40.
- Bijma, J., Hönisch, B., Zeebe, R.E., 2002. Impact of the ocean carbonate chemistry on living foraminiferal shell weight: Comment on "Carbonate ion concentration in glacial-age deep waters of the Caribbean Sea" by W. S. Broecker and E. Clark. *Geochemistry, Geophysics, Geosystems* 3, 1–7.
- Boeckel, B., Baumann, K.-H., 2004. Distribution of coccoliths in surface sediments of the south-eastern South Atlantic Ocean: ecology, preservation and carbonate contribution. *Marine Micropaleontology* 51, 301–320.
- Bolton, C.T., Hernandez-Sanchez, M.T., Fuertes, M.-A., Gonzalez-Lemos, S., Abrevaya, L., Mendez-Vicente, A., Flores, J.-A., Probert, I., Giosan, L., Johnson, J., Stoll, H.M., 2016. Decrease in coccolithophore calcification and  $\text{CO}_2$  since the middle Miocene. *Nat Commun* 7.
- Bostock, H.C., Hayward, B.W., Neil, H.L., Currie, K.I., Dunbar, G.B., 2011. Deep-water carbonate concentrations in the southwest Pacific. *Deep Sea Research Part I: Oceanographic Research Papers* 58, 72–85.
- Boudreau, B.P., 1998. Mean mixed depth of sediments: The wherefore and the why. *Limnology and Oceanography* 43, 524–526.
- Broerse, A.T.C., Ziveri, P., Honjo, S., 2000a. Coccolithophore ( $-\text{CaCO}_3$ ) flux in the Sea of Okhotsk: seasonality, settling and alteration processes. *Marine Micropaleontology* 39, 179–200.
- Broerse, A.T.C., Ziveri, P., van Hinte, J.E., Honjo, S., 2000b. Coccolithophore export production, species composition, and coccolith- $\text{CaCO}_3$  fluxes in the NE Atlantic ( $34^\circ\text{N}21^\circ\text{W}$  and  $48^\circ\text{N}21^\circ\text{W}$ ). *Deep Sea Research Part II: Topical Studies in Oceanography* 47, 1877–1905.
- Brown, C.W., Yoder, J.A., 1994. Coccolithophorid blooms in the global ocean. *Journal of Geophysical Research: Oceans* 99, 7467–7482.
- Caldeira, K., Wickett, M.E., 2003. Oceanography: anthropogenic carbon and ocean pH. *Nature* 425, 365.
- Cao, L., Caldeira, K., 2008. Atmospheric  $\text{CO}_2$  stabilization and ocean acidification. *Geophysical Research Letters* 35 n/a-n/a.
- Charalampopoulou, A., Poulton, A.J., Bakker, D.C., Lucas, M.I., Stinchcombe, M. C., Tyrrell, T.J.B., 2016. Environmental drivers of coccolithophore abundance and calcification across Drake Passage (Southern Ocean), 13. , pp. 5917–5935.
- Connell, R.D., Sikes, E.L., 1997. Controls on Late Quaternary sedimentation of the South Tasman Rise. *Australian Journal of Earth Sciences* 44, 667–675.
- Cook, S.S., Jones, R.C., Vaillancourt, R.E., Hallegraeff, G.M., 2013. Genetic differentiation among Australian and Southern Ocean populations of the ubiquitous coccolithophore *Emiliania huxleyi* (Haptophyta). *Phycologia* 52, 368–374.
- Cook, S.S., Whittock, L., Wright, S.W., Hallegraeff, G.M., 2011. Photosynthetic pigment and genetic differences between two southern ocean morphotypes of *Emiliania huxleyi* (haptophyta). *Journal of phycology* 47, 615–626.
- Cubillos, J., Wright, S., Nash, G., De Salas, M., Griffiths, B., Tilbrook, B., Poisson, A., Hallegraeff, G., 2007. Calcification morphotypes of the coccolithophorid *Emiliania huxleyi* in the Southern Ocean: changes in 2001 to 2006 compared to historical data. *Marine Ecology Progress Series* 348, 47–54.
- Darling, D.A., 1957. The kolmogorov-smirnov, cramer-von mises tests. *The Annals of Mathematical Statistics* 28, 823–838.
- Davis, C.V., Rivest, E.B., Hill, T.M., Gaylord, B., Russell, A.D., Sanford, E., 2017. Ocean acidification compromises a planktic calcifier with implications for global carbon cycling. *Scientific Reports* 7, 2225.
- Dittert, N., Baumann, K.-H., Bickert, T., Henrich, R., Huber, R., Kinkel, H., Meggers, H., 1999. Carbonate dissolution in the deep-sea: methods, quantification and paleoceanographic application, Use of proxies in paleoceanography. Springer, pp. 255–284.
- Ebersbach, F., Trull, T.W., Davies, D.M., Bray, S.G., 2011. Controls on mesopelagic particle fluxes in the Sub-Antarctic and Polar Frontal Zones in the Southern Ocean south of Australia in summer—Perspectives from free-drifting sediment traps. *Deep Sea Research Part II: Topical Studies in Oceanography* 58, 2260–2276.
- Eriksen, R., Trull, T.W., Davies, D., Jansen, P., Davidson, A.T., Westwood, K., van den Enden, R., 2018. Seasonal succession of phytoplankton community structure from autonomous sampling at the Australian Southern Ocean Time Series (SOTS) observatory. *Marine Ecology Progress Series* 589, 13–31.
- Fabry, V.J., McClintock, J.B., Mathis, J.T., Grebmeier, J.M., 2009a. Ocean acidification at high latitudes: the bellwether. *Oceanography* 22, 160.
- Fabry, V.J., McClintock, J.B., Mathis, J.T., Grebmeier, J.M., 2009b. Ocean Acidification at High Latitudes: The Bellwether. *Oceanography* 22, 160–171.
- Feely, R.A., Doney, S.C., Cooley, S.R., 2009. Ocean Acidification Present Conditions and Future Changes in a High- $\text{CO}_2$  World. *Oceanography* 22, 36–47.
- Findlay, C.S., Giraudeau, J., 2000. Extant calcareous nannoplankton in the Australian Sector of the Southern Ocean (austral summers 1994 and 1995). *Marine Micropaleontology* 40, 417–439.
- Findlay, C.S., Giraudeau, J., 2002. Movement of oceanic fronts south of Australia during the last 10 ka: interpretation of calcareous nannoplankton in surface sediments from the Southern Ocean. *Marine Micropaleontology* 46, 431–444.
- Flores, J.A., Sierró, F.J., 1997. A revised technique for the calculation of calcareous nannofossil accumulation rates. *Micropaleontology* 43, 321–324.
- Fuertes, M.-A., Flores, J.-A., Sierró, F.J., 2014. The use of circularly polarized light for biometry, identification and estimation of mass of coccoliths. *Marine Micropaleontology* 113, 44–55.
- Hagino, K., Bendif, E.M., Young, J.R., Kogame, K., Probert, I., Takano, Y., Horiguchi, T., de Vargas, C., Okada, H., 2011. New evidence for morphological and genetic variation in the cosmopolitan coccolithophore *Emiliania huxleyi*

- (prymnesiophyceae) from the COX1b-ATP4 genes. *Journal of Phycology* 47, 1164–1176.
- Hagino, K., Okada, H., Matsuoka, H., 2005. Coccolithophore assemblages and morphotypes of *Emiliana huxleyi* in the boundary zone between the cold Oyashio and warm Kuroshio currents off the coast of Japan. *Marine Micropaleontology* 55, 19–47.
- Iglesias-Rodríguez, M.D., Halloran, P.R., Rickaby, R.E., Hall, I.R., Colmenero-Hidalgo, E., Gittins, J.R., Green, D.R., Tyrrell, T., Gibbs, S.J., von Dassow, P., 2008. Phytoplankton calcification in a high-CO<sub>2</sub> world. *Science* 320, 336–340.
- Jonkers, L., Hillebrand, H., Kucera, M., 2019. Global change drives modern plankton communities away from the pre-industrial state. *Nature* 570, 372–375.
- Kopczynska, E.E., Dehairs, F., Elskens, M., Wright, S., 2001. Phytoplankton and microzooplankton variability between the Subtropical and Polar Fronts south of Australia: Thriving under regenerative and new production in late summer. *Journal of Geophysical Research: Oceans* 106, 31597–31609.
- Krueger-Hadfield, S., Balestreri, C., Schroeder, J., Highfield, A., Helaouët, P., Allum, J., Moate, R., Lohbeck, K.T., Miller, P., Riebesell, U., 2014. Genotyping an *Emiliana huxleyi* (Prymnesiophyceae) bloom event in the North Sea reveals evidence of asexual reproduction. *Biogeosciences* 11, 5215–5234.
- Langer, G., Geisen, M., Baumann, K.-H., Kläs, J., Riebesell, U., Thoms, S., Young, J.R., 2006. Species-specific responses of calcifying algae to changing seawater carbonate chemistry. *Geochemistry, Geophysics, Geosystems* 7 n/a/n-a.
- Langer, G., Nehrke, G., Probert, I., Ly, J., Ziveri, P., 2009. Strain-specific responses of *Emiliana huxleyi* to changing seawater carbonate chemistry. *Biogeosciences* 6, 2637–2646.
- Lenton, A., Tilbrook, B., Law, R., Bakker, D.C., Doney, S.C., Gruber, N., Hoppema, M., Ishii, M., Lovenduski, N.S., Matear, R.J., 2013. Sea-air CO<sub>2</sub> fluxes in the Southern Ocean for the period 1990–2009. *Biogeosciences Discussions* 10, 285–333.
- Manno, C., Bednaršek, N., Tarling, G.A., Peck, V.L., Comeau, S., Adhikari, D., Bakker, D.C.E., Bauerfeind, E., Bergan, A.J., Berning, M.I., Buitenhuis, E., Burrige, A.K., Chierici, M., Flöter, S., Fransson, A., Gardner, J., Howes, E.L., Keul, N., Kimoto, K., Kohnert, P., Lawson, G.L., Lischka, S., Maas, A., Mekkes, L., Oakes, R.L., Pebody, C., Peijnenburg, K.T.C.A., Seifert, M., Skinner, J., Thibodeau, P.S., Wall-Palmer, D., Ziveri, P., 2017. Shelled pteropods in peril: Assessing vulnerability in a high CO<sub>2</sub> ocean. *Earth-Science Reviews* 169, 132–145.
- Mayers, K.M.J., Poulton, A.J., Daniels, C.J., Wells, S.R., Woodward, E.M.S., Tarran, G.A., Widdicombe, C.E., Mayor, D.J., Atkinson, A., Giering, S.L.C., 2019. Growth and mortality of coccolithophores during spring in a temperate Shelf Sea (Celtic Sea, April 2015). *Progress in Oceanography* 177, 101928.
- Metz, N., Tilbrook, B., Poisson, A., 1999. The annual fCO<sub>2</sub> cycle and the air–sea CO<sub>2</sub> flux in the sub-Antarctic Ocean. *Tellus B* 51, 849–861.
- Meyer, J., Riebesell, U., 2015. Reviews and Syntheses: Responses of coccolithophores to ocean acidification: a meta-analysis. *Biogeosciences (BG)* 12, 1671–1682.
- Milliman, J.D., 1975. Dissolution of aragonite, Mg-calcite, and calcite in the North Atlantic Ocean. *Geology* 3, 461–462.
- Milliman, J.D., Troy, P.J., Balch, W.M., Adams, A.K., Li, Y.H., Mackenzie, F.T., 1999. Biologically mediated dissolution of calcium carbonate above the chemical lysocline? *Deep Sea Research Part I: Oceanographic Research Papers* 46, 1653–1669.
- Monahan, J.F., 2011. Numerical methods of statistics. Cambridge University Press.
- Moy, A.D., Howard, W.R., Bray, S.G., Trull, T.W., 2009. Reduced calcification in modern Southern Ocean planktonic foraminifera. *Nature Geosci* 2, 276–280.
- Müller, M.N., Trull, T.W., Hallegraeff, G.M., 2015. Differing responses of three Southern Ocean *Emiliana huxleyi* ecotypes to changing seawater carbonate chemistry. *Marine Ecology Progress Series* 531, 81–90.
- O’Dea, S.A., Gibbs, S.J., Bown, P.R., Young, J.R., Poulton, A.J., Newsam, C., Wilson, P.A., 2014. Coccolithophore calcification response to past ocean acidification and climate change. *Nature Communications* 5, 5363.
- Odate, T., Fukuchi, M., 1995. Distribution and community structure of picophytoplankton in the Southern Ocean during the late austral summer of 1992. *Proc NIPR Symp Polar Biol* 86–100.
- Orr, J.C., Fabry, V.J., Aumont, O., Bopp, L., Doney, S.C., Feely, R.A., Gnanadesikan, A., Gruber, N., Ishida, A., Joos, F., 2005. Anthropogenic ocean acidification over the twenty-first century and its impact on calcifying organisms. *Nature* 437, 681–686.
- Orsi, A.H., Whitworth Iii, T., Nowlin Jr., W.D., 1995. On the meridional extent and fronts of the Antarctic Circumpolar Current. *Deep Sea Research Part I: Oceanographic Research Papers* 42, 641–673.
- Pachauri, R.K., Allen, M.R., Barros, V.R., Broome, J., Cramer, W., Christ, R., Church, J.A., Clarke, L., Dahe, Q., Dasgupta, P., 2014. Climate change 2014: synthesis report. Contribution of Working Groups I, II and III to the fifth assessment report of the Intergovernmental Panel on Climate Change. *Ippc*.
- Pardo, P., Tilbrook, B., van Ooijen, E., Passmore, A., Neill, C., Jansen, P., Sutton, A.J., Trull, T.W., 2019. Surface ocean carbon dioxide variability in South Pacific boundary currents and Subantarctic waters. *Scientific Reports* 9, 7592.
- Patil, S.M., Mohan, R., Shetye, S.S., Gazi, S., Baumann, K.-H., Jafar, S., 2017. Biogeographic distribution of extant Coccolithophores in the Indian sector of the Southern Ocean. *Marine Micropaleontology* 137, 16–30.
- Pearce, I., Davidson, A.T., Thomson, P.G., Wright, S., van den Enden, R., 2011. Marine microbial ecology in the sub-Antarctic Zone: Rates of bacterial and phytoplankton growth and grazing by heterotrophic protists. *Deep Sea Research Part II: Topical Studies in Oceanography* 58, 2248–2259.
- Pearson, K., 1907. On further methods of determining correlation. Dulau and Company.
- Poulton, A.J., Young, J.R., Bates, N.R., Balch, W.M., 2011. Biometry of detached *Emiliana huxleyi* coccoliths along the Patagonian Shelf. *Marine Ecology Progress Series* 443, 1–17.
- Read, B.A., Kegel, J., Klute, M.J., Kuo, A., Lefebvre, S.C., Maumus, F., Mayer, C., Miller, J., Monier, A., Salamov, A., Young, J., Aguilar, M., Claverie, J.-M., Frickenhaus, S., Gonzalez, K., Herman, E.K., Lin, Y.-C., Napier, J., Ogata, H., Sarno, A.F., Shmutz, J., Schroeder, D., de Vargas, C., Verret, F., von Dassow, P., Valentin, K., Van de Peer, Y., Wheeler, G., *Emiliana huxleyi* Annotation, C., Allen, A.E., Bidle, K., Borodovsky, M., Bowler, C., Brownlee, C., Mark Cock, J., Elias, M., Gladyshev, V.N., Groth, M., Guda, C., Hadaegh, A., Debora Iglesias-Rodríguez, M., Jenkins, J., Jones, B.M., Lawson, T., Leese, F., Lindquist, E., Lobanov, A., Lomsadze, A., Malik, S.-B., Marsh, M.E., Mackinder, L., Mock, T., Mueller-Roeber, B., Pagarete, A., Parker, M., Probert, I., Quesneville, H., Raines, C., Rensing, S.A., Riaño-Pachón, D.M., Richier, S., Rokitta, S., Shiraiwa, Y., Soanes, D.M., van der Giezen, M., Wahlund, T.M., Williams, B., Wilson, W., Wolfe, G., Wurch, L.L., Dacks, J.B., Delwiche, C.F., Dyhrman, S.T., Glöckner, G., John, U., Richards, T., Worden, A.Z., Zhang, X., Grigoriev, I.V., 2013. Pan genome of the phytoplankton *Emiliana huxleyi* underpins its global distribution. *Nature* 499, 209.
- Ridgway, K.R., 2007. Seasonal circulation around Tasmania: An interface between eastern and western boundary dynamics. *Journal of Geophysical Research: Oceans* 112.
- Riebesell, U., Zondervan, I., Rost, B., Tortell, P.D., Zeebe, R.E., Morel, F.M.M., 2000. Reduced calcification of marine plankton in response to increased atmospheric CO<sub>2</sub>. *Nature* 407, 364–367.
- Rigual-Hernández, A.S., Trull, T.W., Flores, J.A., Nodder, S.D., Eriksen, R., Davies, D.M., Hallegraeff, G.M., Sierro, F.J., Patil, S.M., Cortina, A., Ballegeer, A.M., Northcote, L. C., Abrantes, F., Rufino, M.M., 2020a. Full annual monitoring of Subantarctic *Emiliana huxleyi* populations reveals highly calcified morphotypes in high-CO<sub>2</sub> winter conditions. *Scientific Reports* 10, 2594.
- Rigual-Hernández, A.S., Trull, T.W., Nodder, S.D., Flores, J.A., Bostock, H., Abrantes, F., Eriksen, R.S., Sierro, F.J., Davies, D.M., Ballegeer, A.M., Fuertes, M.A., Northcote, L. C., 2020b. Coccolithophore biodiversity controls carbonate export in the Southern Ocean. *Biogeosciences* 17, 245–263.
- Rigual Hernández, A.S., Flores, J.A., Sierro, F.J., Fuertes, M.A., Cros, L., Trull, T.W., 2018. Coccolithophore populations and their contribution to carbonate export during an annual cycle in the Australian sector of the Antarctic zone. *Biogeosciences* 15, 1843–1862.
- Rintoul, S., Hughes, C., Olbers, D., 2001. The Antarctic circumpolar current system. In: Siedler, G., Church, J., Gould, J. (Eds.), *Ocean Circulation and Climate*. Academic Press, New York, pp. 271–302.
- Rintoul, S.R., Donguy, J.R., Roemmich, D.H., 1997. Seasonal evolution of upper ocean thermal structure between Tasmania and Antarctica. *Deep Sea Research Part I: Oceanographic Research Papers* 44, 1185–1202.
- Saavedra-Pellitero, M., Baumann, K.-H., 2015. Comparison of living and surface sediment coccolithophore assemblages in the Pacific sector of the Southern Ocean. *Micropaleontology* 61, 507–520.
- Saavedra-Pellitero, M., Baumann, K.-H., Flores, J.-A., Gersonde, R., 2014. Biogeographic distribution of living coccolithophores in the Pacific sector of the Southern Ocean. *Marine Micropaleontology* 109, 1–20.
- Saavedra-Pellitero, M., Baumann, K.H., Fuertes, M.A., Schulz, H., Marcon, Y., Vollmar, N.M., Flores, J.A., Lamy, F., 2019. Calcification and latitudinal distribution of extant coccolithophores across the Drake Passage during late austral summer 2016. *Biogeosciences* 16, 3679–3702.
- Schlitzer, R., 2018. Ocean Data View.
- Schlüter, L., Lohbeck, K.T., Gutowska, M.A., Gröger, J.P., Riebesell, U., Reusch, T.B.H., 2014. Adaptation of a globally important coccolithophore to ocean warming and acidification. *Nature Climate Change* 4, 1024–1030.
- Shadwick, E.H., Tilbrook, B., Cassar, N., Trull, T.W., Rintoul, S.R., 2015. Summertime physical and biological controls on O<sub>2</sub> and CO<sub>2</sub> in the Australian Sector of the Southern Ocean. *Journal of Marine Systems* 147, 21–28.
- Siegel, D.A., Deuser, W.G., 1997. Trajectories of sinking particles in the Sargasso Sea: modeling of statistical funnels above deep-ocean sediment traps. *Deep Sea Research Part I: Oceanographic Research Papers* 44, 1519–1541.
- Siegel, D.A., Granata, T.C., Michaels, A.F., Dickey, T.D., 1990. Mesoscale eddy diffusion, particle sinking, and the interpretation of sediment trap data. *Journal of Geophysical Research* 95, 5305–5311.
- Sikes, E., Howard, W., Samson, C., Mahan, T., Robertson, L., Volkman, J., 2009. Southern Ocean seasonal temperature and Subtropical Front movement on the South Tasman Rise in the late Quaternary. *Paleoceanography and Paleoclimatology* 24.
- Stoll, H.M., Ziveri, P., 2002. Separation of monospecific and restricted coccolith assemblages from sediments using differential settling velocity. *Marine Micropaleontology* 46, 209–221.
- Triantaphyllou, M., Dimiza, M., Krasakopoulou, E., Malinverno, E., Lianou, V., Souvermezoglou, E., 2010. Seasonal variation in *Emiliana huxleyi* coccolith morphology and calcification in the Aegean Sea (Eastern Mediterranean). *Geobios* 43, 99–110.
- Triantaphyllou, M.V., Baumann, K.-H., Karatsolis, B.-T., Dimiza, M.D., Psarra, S., Skampa, E., Patoucheas, P., Vollmar, N.M., Koukousioura, O., Katsigera, A., 2018. Coccolithophore community response along a natural CO<sub>2</sub> gradient off Methana (SW Saronikos Gulf, Greece, NE Mediterranean). *PLoS one* 13, e0200012.
- Trull, T.W., Schulz, E., Bray, S.G., Pender, L., McLaughlan, D., Tilbrook, B., Rosenberg, M., Lynch, T., 2010. The Australian Integrated Marine Observing System Southern Ocean Time Series facility. *OCEANS 2010 IEEE - Sydney*, pp. 1–7.

- Tyrrell, T., Young, J.R., 2009. Coccolithophores. In: Steele, J.H., Turekian, K.K., Thorpe, S.A. (Eds.), *Encyclopedia of Ocean Sciences*. Academic Press, San Diego, pp. 3568–3576.
- van Sebille, E., England, M.H., Zika, J.D., Sloyan, B.M., 2012. Tasman leakage in a fine-resolution ocean model. *Geophysical Research Letters* 39.
- Westbroek, P., Young, J.R., Linschooten, K., 1989. Coccolith Production (Biomineralization) in the Marine Alga *Emiliana huxleyi*. *The Journal of Protozoology* 36, 368–373.
- Young, J., Geisen, M., Cross, L., Kleijne, A., Sprengel, C., Probert, I., Østergaard, J., 2003. A guide to extant coccolithophore taxonomy. International Nannoplankton Association.
- Young, J.R., Ziveri, P., 2000. Calculation of coccolith volume and its use in calibration of carbonate flux estimates. *Deep Sea Research Part II: Topical Studies in Oceanography* 47, 1679–1700.
- Ziveri, P., de Bernardi, B., Baumann, K.-H., Stoll, H.M., Mortyn, P.G., 2007. Sinking of coccolith carbonate and potential contribution to organic carbon ballasting in the deep ocean. *Deep Sea Research Part II: Topical Studies in Oceanography* 54, 659–675.
- Ziveri, P., Rutten, A., de Lange, G.J., Thomson, J., Corselli, C., 2000. Present-day coccolith fluxes recorded in central eastern Mediterranean sediment traps and surface sediments. *Palaeogeography, Palaeoclimatology, Palaeoecology* 158, 175–195.